Mutation Research 793 (2015) 64–70

Contents lists available at ScienceDirect

Mutation Research/Genetic Toxicology and Environmental Mutagenesis

journal homepage: www.elsevier.com/locate/gentox
Community address: www.elsevier.com/locate/mutres

Chromosome aberrations induced by the Auger electron emitter ^{125}I

Sabine Schmitz*, Dominik Oskamp, Ekkehard Pomplun, Ralf Kriehuber

Department of Safety and Radiation Protection, Forschungszentrum Juelich GmbH, 52425 Juelich, Germany

ARTICLE INFO

Article history:
Received 18 August 2015
Accepted 19 August 2015
Available online 24 August 2015

ABSTRACT

DNA-associated Auger electron emitters (AEE) cause cellular damage leading to high-LET type cell survival curves indicating an enhanced relative biological effectiveness. Double strand breaks (DSBs) induced by Iodine-125-deoxyuridine (^{125}I-UdR) decays are claimed to be very complex. To elucidate the assumed genotoxic potential of ^{125}I-UdR, chromatid aberrations were analysed in exposed human peripheral blood lymphocytes (PBL).

PBL were stimulated with medium containing phytohaemagglutinin (PHA). After 24 h, cultures were labelled with ^{125}I-UdR for 18 h (activity concentration 1–45 kBq) during the S-phase. Following standard cytogenetic procedure, at least 100 metaphases were analysed microscopically for each activity concentration. Cell death was measured by apoptosis assay using flow cytometry. Radiation doses were determined by using point kernel calculations.

After 18 h labelling with ^{125}I-UdR the cell cycle distribution is severely disturbed. About 40% of PBL are fully labelled and 20% show a moderate labelling of ^{125}I-UdR, whereas 40% of cells remain un-labelled. The dose-response relationship fits to a polynomial curve in the low dose range, whereas a linear fit supplies a better estimation in the high dose range. Even the lowest dose of 0.2 Gy leads to a 13-fold increase of aberrations compared to the controls. On average every fifth ^{125}I-decay produces a single chromatid aberration in PBL. Additionally, a dose-dependent increase of cell death is observed.

^{125}I-UdR has a very strong genotoxic capacity in human PBL, even at 0.2 Gy. Efficiently labelled cells displaying a prolonged cell cycle compared to moderately labelled cells and cell death contribute substantially to the desynchronisation of the cell cycle. Our data, showing for the first time, that one ^{125}I-decay induces ~ 0.2 chromatid aberrations, are in very good accordance to DSB data, stating that ~0.26 DSB are induced per decay, indicating that approximately every DSB is converted into a chromatid aberration.

1. Introduction

Since the first demonstration of strong radiotoxic effects induced by the DNA incorporated Auger electron emitter (AEE) ^{125}I [1,2], this special class of radionuclides has attracted great attention by radiobiologists. Due to their particular particle emission spectra, these nuclides offer a unique possibility to irradiate specific cellular target structures without damaging neighboring cells and tissues. In purified DNA, more than 70% of strand breaks were induced within less than five base pairs from the decay site of ^{125}I corresponding to about 20 angstroms (Å) [3]. By a successful simulation of the electron tracks in combination with a DNA volume model [4], this strongly localized damage could be ascribed to the emission of a shower of low energy short-ranging Auger electrons. A mean number of approximately one dozen of these electrons are released per ^{125}I-decay [5]. Meanwhile, ^{125}I is certainly the most prominent radionuclide among AEE (see review [6]). During the last four decades many experimental and theoretical studies have been performed to elucidate the impact of the emitted Auger electrons on different biological targets like plasmid DNA, bacteriophages and cell cultures [6–10].

For the understanding of the biological impact of AEE, the cellular location is of crucial importance [7]. Whereas ^{125}I-decay events in the plasma membrane caused only minimal cell damage [8], decays in the cytoplasm turned out to be ineffective with regard to cell killing [9]. From ^{125}I-decays located in mitochondrial DNA it is known that extra-nuclear DNA is not a sensitive target for cell death induction [10].

However, ^{125}I-carrier-conjugates proved to be a useful tool since these vehicles are internalised by cells. After the up-take

* Corresponding author at: Department of Safety and Radiation Protection Radiobiology, Forschungszentrum Jülich GmbH, D-52425 Jülich,Germany. Fax: +49 2461 61 3726.
E-mail address: sa.schmitz@fz-juelich.de (S. Schmitz).

http://dx.doi.org/10.1016/j.mrgentox.2015.08.007

of an antibody-^{125}I-conjugate into large cytoplasmic vesicles (macropinosomes), the observed cytotoxic effect was associated with the observation that the vesicles are often located close to the nucleus [11]. In another experimental approach, an ^{125}I-estrogen/estrogen receptor-complex was used to irradiate the nucleus by binding specific DNA sequences called estrogen response elements (EREs). As a consequence, a 4.5-fold higher cell killing efficiency was found when compared to γ-irradiation [12]. Finally, ^{125}I-labelled Triplex-forming oligonucleotides (TFOs) leading to site-specific breaks in genomic DNA, demonstrated that double strand break (DSB) efficiency is strongly correlated with proximity to a nuclear target [13]. All these observations lead to the current view that ^{125}I, located in a non-nuclear target, has only minor consequences for the cell, whereas the strongest impact is observed when the radionuclide is within or in close proximity to nuclear DNA.

From comparative studies it is known that decays of ^{125}I-UdR lead to survival curves with no or very small shoulder in contrast to other radionuclides displaying a wide shoulder [14]. The detected differences evoked the question what kind of molecular damage caused the observed differences in cell survival. It was supposed that there is a close correlation between lethality and DNA breaking efficiency and that cell death is a result of unrepaired DNA damage. Thus, the greater radiotoxicity of ^{125}I-UdR was associated to its strong capacity to cause DSBs, underlining its mode of action as a high LET-radiator.

First experiments investigating the DSB induction showed that on average one ^{125}I-decay produced one DSB in bacteriophage T4 [15]. Further analyses in mammalian cells like human fibroblasts were performed and comparable results were obtained [16]. However, slight differences in DSB production might be explained by the considerably higher complexity of the mammalian genome compared to the bacteriophage viral genome and due to other factors modulating DSB damage induction by ^{125}I-decay.

To investigate this biological endpoint more intensely, scientists searched for exact and reliable methods for the quantification of DSBs. Hence, a new assay for the indirect detection of γH2AX foci turned out to be an appropriate tool [17,18]. This assay represents a novel approach for the rapid estimation of radiation-induced DNA lesions based on the ratio that one focus represents one DSB. The DSBs induced by ^{125}I-UdR-decays are described to be very complex, due to a high degree of base damages clustered proximal to the DSB end. Thus, DNA-associated Auger electron emitters like ^{125}I-UdR are assumed to possess a pronounced genotoxic potential because of their capability to induce considerable damage, which challenges the cells' repair mechanisms due to this complex nature of the produced breaks [19,20].

Although complex DSBs are known to cause chromosome aberrations (CA), only few data exist for aberrations induced by ^{125}I-UdR. Most of them were obtained analyzing either adherent human fibroblasts or permanent cancer cell lines. In this study, for the first time, the induction of CA due to the DNA-associated AEE ^{125}I-UdR was investigated to elucidate the genotoxic potential of ^{125}I in stimulated primary human lymphocytes. This work provides additional information about why decays of ^{125}I-UdR induce high LET-type damages and cell killing and how the decays are converted into CA.

2. Material and methods

2.1. Isolation of lymphocytes from whole blood

Blood samples were drawn by venipuncture from a voluntary healthy male donor. Peripheral blood lymphocytes (PBL) were isolated using the BD Vacutainer CPT™ System with Sodium Heparin (BD Biosciences, Heidelberg, Germany) according to the manufacturer's recommendations. The cell number was determined out of 1 mL cell suspension using a CASY Counter TTC (Roche, Penzberg, Germany). Until onset of experiments, cells were cultured in RPMI 1640 medium with 2% stable glutamine (Roswell Park Memorial Institute; PAA, Pasching, Austria), 20% fetal bovine serum (FBS, Biochrom, Berlin, Germany) and 1% antibiotics (PAA, Pasching, Austria). Cell cultures were incubated in a 5% CO_2 gassed humidified incubator (Sanyo Biomedical, Bad Nenndorf, Germany) at 37 °C. 3 h after isolation, cells were centrifuged and then cultured in chromosome medium B with PHA (phytohaemagglutinin; Biochrom, Berlin, Germany). Between 3–3.5 × 10^6 cells per 10 mL culture were set up each for the control and the samples exposed to increasing activities of ^{125}I-UdR.

2.2. Labelling of PBL with ^{125}I-UdR, determination of cell number and measurement of incorporated ^{125}I-activity

24 h after PHA stimulation PBL were labelled with ^{125}I-UdR (total activity concentration 1–45 kBq; Perkin Elmer, Boston, USA) for 18 h. To optimize the uptake and the incorporation of ^{125}I-UdR into the cells iododeoxyuridine (IUdR), 5-fluoro-2'-deoxyuridine (FUdR) and 2-deoxycytidine (CdR, Fluka, Sigma–Aldrich, Munich, Germany) were added to each culture at a concentration equivalent to the molar concentration of radiolabelled ^{125}I-UdR used (10^{-8} M). Labelling was terminated after 18 h by removing the medium after centrifugation. After washing cells twice with PBS, activity measurement was determined in 1 mL cell suspension in PBS using the 1480 Automatic Gamma Counter Wizard™ 3″ (PerkinElmer, Rodgau-Jügesheim, Germany). The cell number was determined out of the same cell suspension using a CASY Counter TTC. The cells were then centrifuged and cultured again in 5 ml fresh chromosome medium B. Colcemid™ (final concentration 0.03 μg/mL; PAA, Pasching, Austria) was added 5.5 h before harvest.

2.3. Click-iT® EdU Flow cytometry cell proliferation assay

To determine the ^{125}I-UdR incorporation into the replicating DNA of proliferating PBL, the Click-iT® EdU Flow cytometry cell proliferation assay (Life technologies, Invitrogen, Karlsruhe, Germany) was performed and set up in parallel to the sample exposed to the highest activity in each experiment. The assay was performed after radioactive labelling of PBL was terminated at 42 h of culture and at 72 h for control of incorporation kinetics according to the manufacturer's recommendations. Briefly, samples containing EdU (5-ethynyl-2′-deoxyuridine, final concentration 500 nM) were labelled with ^{125}I-UdR for 18 h. After removal of the radioactive medium and washing steps, cell counts and activity were determined. EdU samples were fixed with 4% PFA/PBS (paraformaldehyde) for 15 min, at RT (room temperature). Cell pellet was blocked with wash buffer (1% BSA/PBS, bovine serum albumin) and then permeabilized in Saponin based permeabilization and wash buffer for 15 min, at RT. Samples were transferred to flow cytometry tubes and incubated with Click-iT Reaction Cocktail for 30 min, at RT in the dark. After centrifugation the pellet was resuspended in RNAse A (final concentration 0.1 mg/mL) and incubated for 10 min, at 37 °C. Subsequently, cells were washed with 1xSSC/0.1 % Triton X-100. The cell pellet was stained with Sytox Green (0.1 μM) for 10 min, at RT in the dark. Finally, the EdU containing sample was measured using a FACSCanto II™ flow cytometer (BD Biosciences, Heidelberg, Germany).

2.4. FITC Annexin V Apoptosis assay

The FITC Annexin V Apoptosis Detection Kit I (BD Pharmingen™, Heidelberg, Germany) was used to determine quantitatively the

percentage of cells that are actively undergoing apoptosis within the control sample and the ^{125}I-UdR labelled samples. Approximately 1×10^6 cells per mL were washed twice with cold PBS, followed by centrifugation at $300 \times g$ for 5 min. Cells were resuspended in 1x binding buffer. Then 100 μL of the solution (1×10^5 cells) was transferred to a culture tube and 5 μL of FITC Annexin V and 5 μl PI (propidium iodide) was added. Cells were vortexed and incubated for 15 min at RT in the dark, followed by addition of 400 μL 1x binding buffer. Finally, samples were analysed by flow cytometry within 1 hour using a FACSCanto II^{TM} flow cytometer.

2.5. Cell fixation and scoring of aberrations

PBL were harvested according to a cytogenetic standard procedure. Cells were incubated in 0.075 M KCl (Merck, Darmstadt, Germany) solution at 37 °C for 15 min and fixed in 3:1 methanol: acetic acid solution (Merck, Darmstadt, Germany). Thereafter, cells were dropped on clean fat-free slides (Geyer, Renningen, Germany) and stained with 10% Giemsa diluted in microscopy buffer (Weise buffer) pH 6.8 (both Merck, Darmstadt, Germany). All types of aberrations detected were added together to give the final aberration score for both irradiated and control samples. At least 100 metaphases were scored microscopically per activity concentration in each experiment. ^{125}I-UdR-induced aberrations in a dose range from 0.2 to 3.8 Gy (corresponding to 1–45 kBq) were analysed. In total, 5500 metaphases were evaluated for the dose-response relationship. Data points were summarized in 0.5 Gy dose increments to obtain more data at one data set.

2.6. Dose calculation

The particle emission spectra of AEE represent a complex challenge with regard to radiation dosimetry. To determine the radiation dose in case of the DNA-incorporated AEE ^{125}I, the characteristic energy deposition patterns of the short-ranging Auger electrons have to be kept in mind. Most of these electrons possess energies below 5 keV and therefore ranges in tissue below one micrometer [5]. In addition, the electron emission spectrum of ^{125}I [5] includes at least some electrons with energies and, respectively, ranges of about 15 μm being able to escape from DNA structures into the cell nucleus. So, the energy deposition to the DNA alone might not be sufficient to explain cellular damage. Moreover, it has been demonstrated in numerous experiments that the dose to the cell nucleus can be seen as a reasonably good predictor for the assessment of radiation damage (for a detailed discussion, see e.g. [21]).

Based on the activity and cell number measurements (see Section 2.2) the accumulated number of decays per cell was calculated. The dose to the cell nucleus per ^{125}I-decay was determined for a spherical volume of 7.5 μm, the assumed average diameter of a lymphocyte nucleus, to be 6.8 mGy. The total dose is then given by multiplication of this value with the number of decays which in turn corresponds to the administered activities of ^{125}I-UdR.

3. Results

3.1. Type and frequency of chromosome aberrations induced by ^{125}I-UdR

After incorporation of ^{125}I-UdR into PBL primarily chromatid-type aberrations are observed. Over the whole dose range screened in this study, the frequency distribution of the aberration types found did not change significantly. In the low as well as in the high dose range (3.1–3.5 Gy) the most frequently found types were simple aberrations like breaks and gaps. As shown in Fig. 1, a mean of

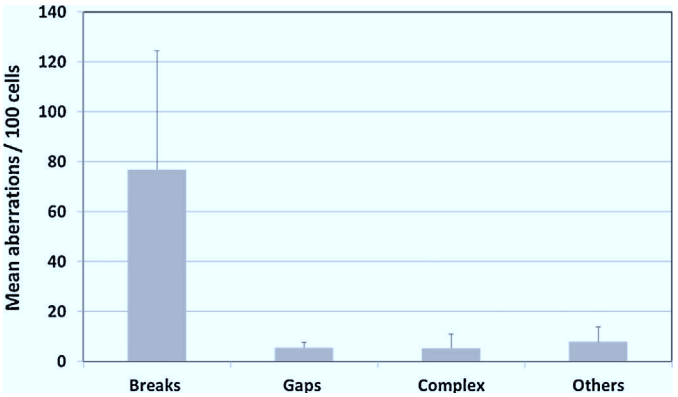

Fig. 1. Frequency of chromatid-type aberrations induced in PBL after incorporation of ^{125}I-UdR in the dose range 3.1–3.5 Gy ($N = 5$). Error bars represent the standard deviation (SD).

76.9 breaks per 100 cells were detected, demonstrating that chromatid breaks are by far the most frequent aberration type. All other types of chromatid aberrations like complex (5.4/100 cells), gaps (5.6/100 cells) and other aberrations like fragments and minutes (7.9/100 cells) range in a comparable level. Complex aberrations like triradial and quadriradial chromosomes are created when 2 chromosomes are involved and the repair of their chromatid breaks failed. The result of this misrepair is an asymmetrical chromatid interchange representing the complex chromatid-type aberration. Our data indicate that ^{125}I-UdR induces simple rather than complex chromatid aberrations.

Representative images of metaphases analysed for chromosome aberrations are shown in Fig. 2. In control metaphases generally no or only few spontaneous aberrations could be detected (2A). After exposure to a moderate dose (0.7 Gy) mainly simple aberrations like gaps and breaks were found (2B), whereas at a dose of 1.3 Gy, simple as well as complex aberrations were observed (2C). Metaphases exposed to 3 Gy contained multiple complex damages which were hardly quantifiable (2D). Those metaphases occurred predominantly in the dose range between 3 and 3.8 Gy.

3.2. Dose-response relationship for ^{125}I-UdR-induced chromosome aberrations

In general, the data demonstrate that even the lowest dose of 0.2 Gy leads to significant damage and to a 13-fold significant increase of aberrations compared to the controls, showing a mean of 2.4 spontaneous aberrations. The dose-response-relationship can be described by using a polynomial as well as a linear fit (Fig. 3). The polynomial dose-response curve ($Y = -13.11 \times 2 + 88.10x + 2.43$; $R2 = 0.72$) exhibits a continuous increase of aberrations up to 3 Gy, followed by a plateau between 3 Gy and 3.8 Gy. When fitted linearly, the dose-response relationship is described by $Y = 48.72x + 2.43$; $R2 = 0.58$. In the dose range 0.2–3 Gy the linear fit is slightly below the polynomial curve. In the higher dose range above 3 Gy polynomial and linear fit differ significantly.

From the measurement of cell numbers, decays per cell nucleus and scored aberrations, we calculated that on average every fifth decay of ^{125}I-UdR in the DNA induced one chromatid aberration in human PBL, or more specifically, one decay produced 0.2 chromatid aberrations.

3.3. Cell cycle progression and radiation-induced loss of cells

After 18 h labelling with ^{125}I-UdR the cell cycle distribution is severely disturbed. About 40% of PBL are fully labelled and 20 %

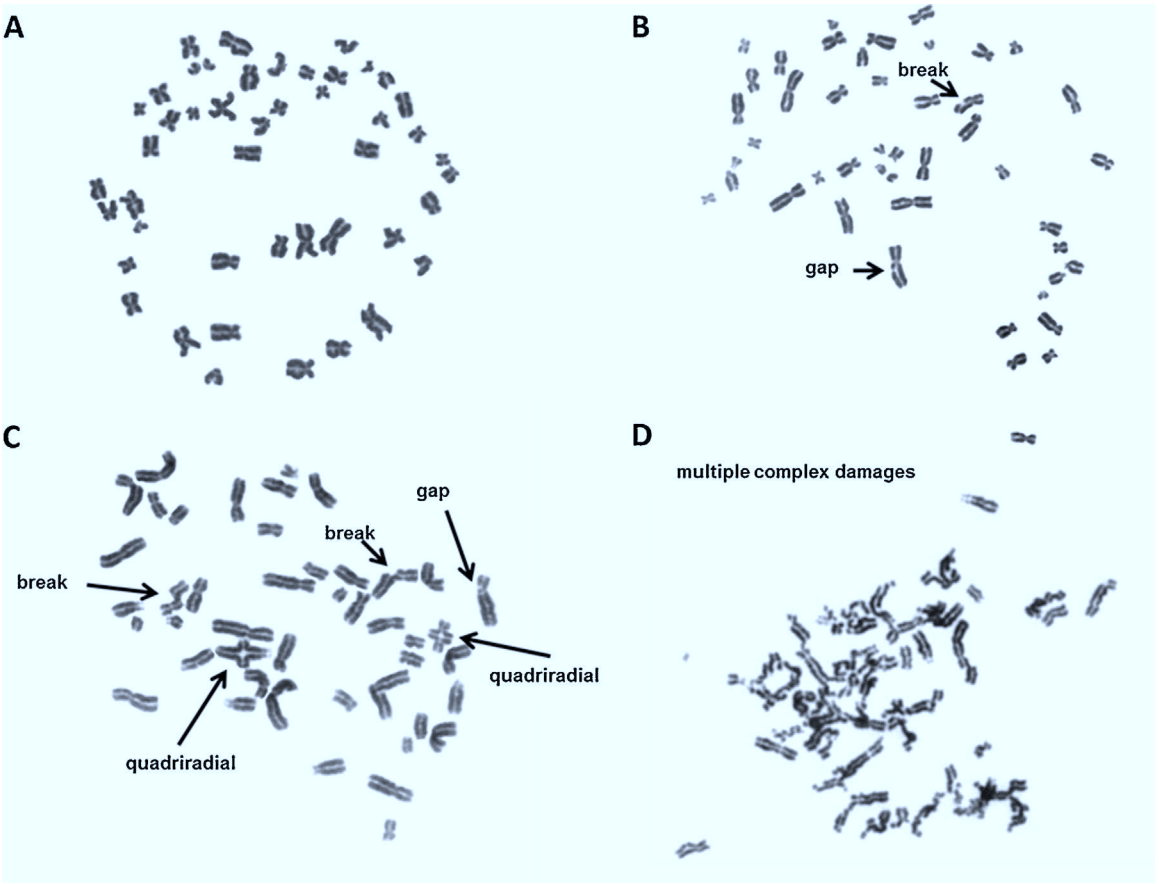

Fig. 2. DNA damage response following incorporation of ^{125}I-UdR into human PBL. (A) Control metaphase without any aberration. (B) Moderately damaged metaphase showing simple chromatid-type aberrations like gaps and breaks. (C) Severely damaged metaphase demonstrating simple and a complex aberrations like quadriradial chromosomes. (D) Highly damaged metaphase with a non-quantifiable level of chromatid aberrations.

show a moderate labelling of ^{125}I-UdR, whereas 40% of cells remain un-labelled, because they did not enter the cell cycle. Cell numbers were measured in each sample initially before PHA stimulation and immediately after termination of labelling with ^{125}I-UdR. Thus, the progression of the cell numbers was observed over a time period of 42 h, reflecting a pronounced ^{125}I-UdR-induced cell death observed in human PBL (data not shown).

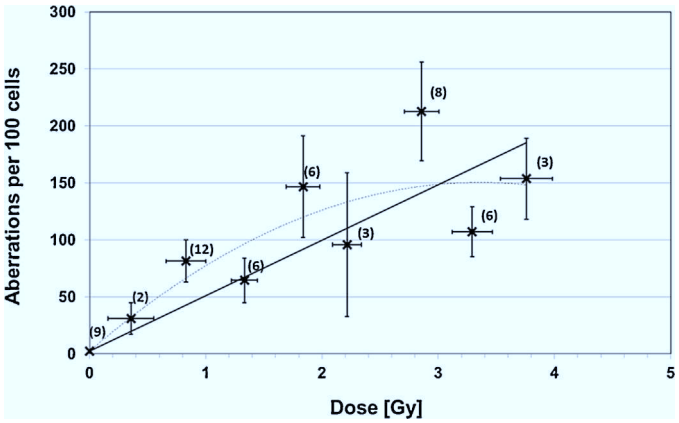

Fig. 3. Dose response relationship for chromosome aberrations induced by ^{125}I-UdR (N = 9).
⊥ = standard deviation (SD).
⊢ = standard error of the mean (SEM).

3.4. Apoptosis measurement in controls and in ^{125}I-labelled PBL

Apoptosis was measured at several time points (0, 24, 48, 66 and finally 70 h) during the whole experimental procedure. The initial proportion of apoptosis was determined immediately after isolation of PBL and then after 24 h of PHA stimulation. From Fig. 4, it can be seen that in the controls more than 70% of cells were viable and there were approximately equal amounts (~13%) of apoptotic and necrotic cells found directly after isolation of cells by density centrifugation (0 h). After 24 h of PHA stimulation viable cells further decrease to less than 60% whereas the amount of both apoptotic and necrotic control cells together increases to about 40% (Fig. 4A–C). Whereas in control cells apoptosis and necrosis significantly decrease over time leading to approximately 80% viable cells, the ratio of ^{125}I-UdR irradiated but viable cells is in the range of only 50–68% after incorporation of 10 kBq and 60–52% after 40 kBq (Fig. 4A).

Apoptotic as well as necrotic cells in the controls decrease over time to about 10–12% after 70 h (Fig. 4B–C). Cells that have incorporated 10 kBq of ^{125}I-UdR show an increase of apoptosis until 66 h followed by a slight decrease at 70 h. After incorporation of 40 kBq an increase up to 27% apoptosis could be found. In general, irradiated PBL display a dose dependent increase of apoptosis between 48 h and 70 h (Fig. 4B).

At 48 h after culture set up, the proportion of necrosis in those cells that incorporated 10 kBq increased to 24% but decreased at 66 h to 17% and further at 70 h to 13%, respectively. After 40 kBq ^{125}I-UdR the proportion of necrosis is approximately constant over time ranging from 15 to 17% (Fig. 4C).

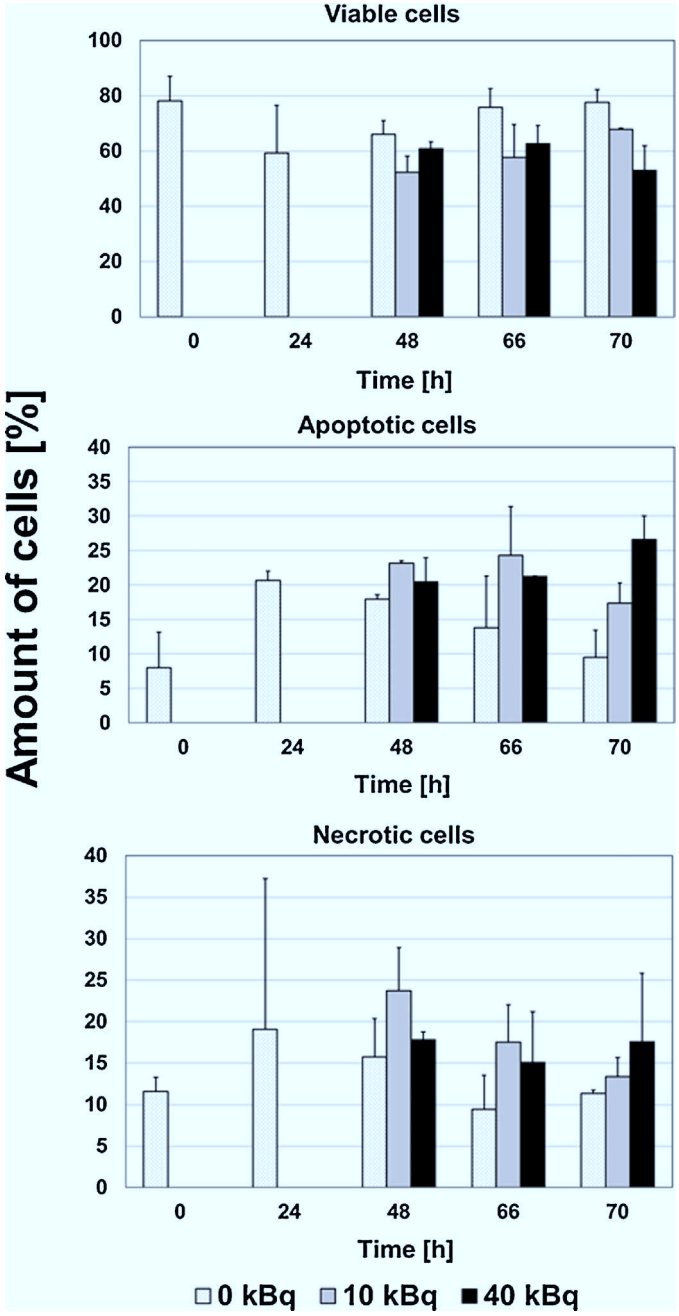

Fig. 4. Percent of viable (A), apoptotic (B) or necrotic (C) cells at different time points: after isolation (0 h) of PBL, after stimulation with PHA and before incubation with ^{125}I-UdR (24 h), after removing of ^{125}I-UdR (48 h), immediately before addition of Colcemid (66 h) and before harvesting (70 h) of PBL ($N = 3$). Error bars represent the standard deviation (SD).

4. Discussion

4.1. Type and frequency of chromatid aberrations induced by ^{125}I-UdR

In this study ^{125}I-UdR was incorporated in human PBL for 18 h during S-phase. It is known that in S-phase both types of aberrations (chromosome and chromatid-type aberrations) can occur, depending on whether the damaged DNA is already replicated or not. Our data indicate that ^{125}I-UdR-induced DNA damage is primarily produced at the onset of S-phase when the DNA is not yet replicated, thus resulting in chromatid-type aberrations. Among these, much more simple type aberrations as breaks and gaps than complex type aberrations like tri- and quadriradial chromosomes were induced by decays of ^{125}I-UdR (Fig. 1). Possibly, quadriradials (as shown in Fig. 2C) occurred less frequently because at least two chromatid breaks in neighboring chromosomes induced at the same time followed by their misrepair are required to generate such an asymmetrical chromatid interchange. Although in our study such configurations occurred rarely, it cannot generally be excluded that complex aberrations occurred anyhow, but primarily in highly damaged cells (Fig. 2D).

Cells exhibiting a critical amount of lethal damages were not detectable in the assay due to ^{125}I-UdR-induced extensive cell death (discussed in more detail in Section 4.3). Thus, the main aberration type found was the chromatid break with 76.9% versus 5.4% complex aberrations. Our results are in good agreement with data from Sundell-Bergman et al. [22], especially because these authors used the same labelling scheme and a comparable experimental procedure. They labelled Cl:1 cells for 18 h at 37 °C with ^{125}I-UdR and found less than 10% exchanges compared to all other types of chromatid aberrations scored. Although DNA lesions are already repaired during labelling time, a considerable amount of residual chromatid breaks were detected even after low doses as 0.2 Gy. This observation points out that the type of DSB caused by ^{125}I-UdR is structurally more complex and therefore comparable with clustered high LET-type damage [23]. Our findings are therefore in line with data described by Datta et al. [19], who analysed radiation-induced DSBs using an in vitro model of plasmid DNA linearised by an ^{125}I-labelled triplex-forming oligonucleotide (TFO). These authors conclude that DSBs produced by ^{125}I-TFO exhibit a high degree of clustered base damages in the proximity of the DSB end and they assume that those damages may be a major factor leading to the less successful in vitro repair by the non-homologous end joining pathway (NHEJ). Additionally, ^{125}I-labelled TFO were shown to induce sequence specific complex DNA lesions and specific alterations of gene expression, underlining its capacity to significantly increase the number of DSBs in targeted genes [24].

As it is known that DNA damages produced during S-phase can be repaired by NHEJ as well as by homologous recombination (HR), mammalian cells have more than one option to repair DNA lesions. Nevertheless, the fact that even in the low dose range considerable residual damage was observed, points to repair problems associated with the complex nature of the DSBs provoked by ^{125}I-UdR. Our chromosome data support the hypothesis that DNA associated AEE like ^{125}I-UdR lead to high LET-type damage as it was postulated by Hofer et al. [25]. Two reasons seem to be responsible for the experimental findings: ^{125}I-UdR is a potent inducer of clustered DSBs due to its physical properties as already mentioned in the introduction. Additionally, the structural nature of the DSBs produced is complex due to clustered base damages in the proximity of the break ends. Both together lead to a kind of DNA lesion that challenges the cells' repair machinery.

4.2. Dose-response relationship of ^{125}I-UdR induced chromosome aberrations

The question of the dose-response relationship is not easily answered. Because two regression models seem to fit to our data, a differentiated consideration is needed.

4.2.1. The polynomial fit

The curve progression of the polynomial fit reflects exactly the actually measured data. The initial increase of aberrations caused by ^{125}I-UdR is followed by a plateau phase. The plateau expresses the extensive cell death occurring in the higher dose range when cells have accumulated lethal damages. The data are in good agreement with the apoptosis measurements providing

experimental evidence, that the considerable cell death especially in the dose range 3.1–3.8 Gy (corresponding to activity concentrations of 20–45 kBq), is obviously caused by apoptosis. Thus, the plateau can be conclusively explained by the loss of highly labelled cells.

Nevertheless, we are aware that particularly in this dose range measuring inaccuracies occur, which are associated with the difficulty to score aberrations in highly damaged cells. Hence, the plateau of the curve might reflect an underestimation of the actual amount of aberrations, due to scoring errors and additionally, and more important, the loss of highly damaged cells. Furthermore, the data set at 3.8 Gy consists of only 3 data points, whereas most other data sets are composed of many more data points. Especially the last data set at 3.8 Gy drives the polynomial curve into the plateau.

4.2.2. The linear fit

Due to the above discussed reasons for the plateau at doses >3 Gy we decided to give a linear fit of the data. The linear dose-response relationship underestimates the aberration score in the low dose range, but it probably provides for a better estimation in the high dose range. Especially above 3 Gy, it considers the loss of highly labelled cells due to apoptosis/necrosis and the amount of non-quantifiable metaphases of heavily damaged cells. Thus, the linear fit represents a conservative estimation of ^{125}I-UdR-induced aberrations providing an appropriate reflection of the data accuracy in the high dose range.

4.2.3. Final remarks

Different dose-response relationships for chromosome aberrations are described in the literature, depending on the radiation quality. Whereas low LET radiations like γ- and X-rays show a non-linear curve [26], for high LET radiation linear response curves were found by Lee et al. [27] and are also reviewed by Ritter & Durante [28]. The dose-response relationship of aberrations induced by ^{125}I-UdR fits to a polynomial as well as to a linear model in the low dose range. In the high dose range (beyond 3 Gy) the linear model fits better, because it considers the measuring inaccuracies associated with the scoring of aberrations in highly damaged cells, which are very often not accurately quantifiable. Interestingly, a plateaued dose-response relationship was found by Yasui [18] for the induction of ^{125}I-UdR-induced γH2AX foci in the breast cancer cell line MCF7. The author describes a plateau for the average number of γH2AX foci at ^{125}I-decays greater than 200 decays per cell. The found number of foci was 0.26 foci per decay and thus turned out to be lower than expected when compared to data from Krisch & Ley [15] obtained with bacteriophage T4. Comparable results were also reported by Sedelnikova et al. [17], who found 0.3 foci per decay in asynchronous HT-1080 cells and 0.24 foci per decay in SF-268 cells. Due to combination of our own data and the results of Yasui [18] and Sedelnikova et al. [17] it can be concluded that in human lymphocytes per ^{125}I-decay approximately 0.26 DSBs are induced resulting in 0.2 chromatid aberrations. Thus, our findings of ^{125}I-UdR induced chromatid aberrations are in line with the results of these authors for the induction of γH2AX foci, and strongly indicate that almost every DSB caused by ^{125}I-UdR is converted into a chromatid aberration.

4.3. Cell cycle progression, residual damage and ^{125}I-UdR-induced cell killing

The incorporation of ^{125}I-UdR during S-phase affects the progression of cells through the cell cycle. Efficiently labelled cells displaying a prolonged cell cycle compared to moderately labelled cells, and cell death contribute substantially to the observed desynchronisation of the cell cycle. This observation demonstrates that cell cycle delay is initiated already at the beginning of the labelling procedure. Because cells are damaged throughout the whole labelling period, lesions induced at early S-phase might not be repaired when further damages are accumulated during late S-phase. This leads to a persistent level of DNA damage, finally resulting in a high level of residual unrepaired breaks found even after low doses of ^{125}I-UdR. These residual damages are supposed to be lethal for the cell. Several authors [29,30] described that residual damage represents a subset of DSB that cannot quickly be repaired or rejoined. Their persistence over a longer period of time is suggested to be an indicator of cell killing probability [31]. A dose-dependent increase of cell loss is also observed in this study after incorporation of ^{125}I-UdR. Our data are in agreement with these authors and therefore underline the higher cell killing efficiency of high LET-type damages caused by ^{125}I-decays.

4.4. Conversion of ^{125}I-UdR induced DNA damage into chromatid breaks

The precise mechanism for the induction of chromosomal damage following radiation is still the subject of a long-standing controversy in radiation cytogenetics. However, new insights in the formation of radiation-induced chromosome aberrations came from direct observation of interphase chromatin leading to a changed view on the role of chromatin dynamics during the cell cycle as recently issued by Pantelias & Terzoudi [32]. As a result, a new hypothesis was formulated by Terzoudi et al. [33] concerning the conversion of DNA damage into chromatid breaks. These authors discuss a strong association of the formation of chromatid breaks with chromatin dynamic changes in the presence of DNA damage. They argue that chromatid breaks are not always the result of inefficient DNA repair pathways, but rather of the biophysical process exerted by the inherent mechanical stress of chromosomal conformation changes that converts DNA damage into chromatid breaks before DSBs or other lesions are completely repaired. These arguments seem to be of great importance for the irradiation situation described in our study. As cells were labelled with ^{125}I-UdR at the onset of S- phase, resulting DNA damages occurred when cells changed their chromatin dynamics to allow DNA replication. Moreover, cells accumulate further lesions during the remaining 18 h of labelling time leading to a persistent and cumulative DNA damage level. Terzoudi et al. [33] proposed that the conversion of DNA damage into chromatid breaks is cell cycle dependant and functions in an antagonistic way to DNA repair processes. That means that even under efficient repair pathways like HR which is operating in S-phase, structural and functional features of chromatin might interact and affect the processes involved in repair or misrepair of initially induced damage.

Similar conclusions were already reported by Elmroth & Stenerlöw [34] who found non-random DNA fragmentation after irradiation with ^{125}I. They detected significantly more ^{125}I-induced DSBs in late rather than in early S-phase and explain their result with different chromatin organization.

Thus, the type and yield of radiation-induced damage is proposed to be the result of two counteracting processes: mechanical stress due to abrupt chromatin dynamic changes during S-phase on the one hand and cellular efforts to repair ^{125}I-UdR-provoked chromatid breaks on the other hand. These considerations seem to be a plausible explanation for the high level of unrepaired breaks found even after low doses of ^{125}I-UdR in this study. Finally, how these processes interact on the molecular level has to be investigated by further analyses.

5. Summary

^{125}I-UdR decays induce simple rather than complex chromatid-type aberrations in human PBL. The dose-response relationship

in the low dose range fits well to a polynomial curve since it exactly reflects the measured data. In the high dose range (beyond 3 Gy) the linear model fits better, because it considers the measuring inaccuracies associated with the scoring of aberrations in highly damaged cells, which are very often not accurately quantifiable. The extensive cell death observed is due to those cells bearing a critical amount of unrepaired breaks, representing accumulated lethal damages due to high activity concentrations of ^{125}I-UdR. Our results demonstrate that cells die due to apoptosis. We calculated that every fifth ^{125}I-decay inside the DNA leads to a chromatid aberration which was less than expected due to data obtained from bacteriophage T4. Considering the DSB data from Yasui [18] and Sedelnikova et al. [17], who showed that one ^{125}I-decay induced 0.26 detectable γH2AX foci, we can conclude that every ^{125}I-induced DSB is converted into a chromatid aberration due to impaired repair processes, probably caused by the structural complex nature of clustered DSBs. Furthermore, we point out that chromatin dynamics may play an important role for the conversion of DNA damage into chromatid breaks induced by ^{125}I-UdR.

Conflict of interest

The authors declare that there are no conflicts of interest.

Acknowledgements

The authors thank M. von Ameln for very helpful support in scoring of aberrations.

This work was funded by Dr.-Erich-Schmitt-Stiftung and BMBF Grant 02NUK005A.

References

[1] K.G. Hofer, W.L. Hughes, Radiotoxicity of intranuclear tritium, 125 iodine and 131 iodine, Radiat. Res. 47 (1971) 94–109.
[2] L.E. Feinendegen, E. H.H., B. V.P., Biological toxicity associated with the Auger effect, in: E. H. (Ed.) Symposium on Biophysical Aspects of Radiation Quality, IAEA, Vienna, 1971, pp. 419-430.
[3] R.F. Martin, W.A. Haseltine, Range of radiochemical damage to DNA with decay of iodine-125, Science 213 (1981) 896–898.
[4] D.E. Charlton, J.L. Humm, A method of calculating initial DNA strand breakage following the decay of incorporated ^{125}I, Int. J. Radiat. Biol. Relat. Stud. Phys. Chem. Med. 53 (1988) 353–365.
[5] E. Pomplun, Auger electron spectra–the basic data for understanding the Auger effect, Acta Oncol. 39 (2000) 673–679.
[6] The 7th International Symposium on Physical, Molecular, Cellular, and Medical Aspects of Auger Processes, International journal of radiation biology, 2012, pp. 861-1045.
[7] R. Kriehuber, M. Riedling, M. Simko, D.G. Weiss, Cytotoxicity, genotoxicity and intracellular distribution of the Auger electron emitter (65)Zn in two human cell lines, Radiat. Environ. Biophys. 43 (2004) 15–22.
[8] R.L. Warters, K.G. Hofer, Radionuclide toxicity in cultured mammalian cells. Elucidation of the primary site for radiation-induced division delay, Radiat. Res. 69 (1977) 348–358.
[9] K.G. Hofer, C.R. Harris, J.M. Smith, Radiotoxicity of intracellular ^{67}Ga, ^{125}I and ^{3}H. Nuclear versus cytoplasmic radiation effects in murine L1210 leukaemia, Int. J. Radiat. Biol. Relat. Stud. Phys. Chem. Med. 28 (1975) 225–241.
[10] L.S. Yasui, K.G. Hofer, Role of mitochondrial DNA in cell death induced by ^{125}I-decay, Int. J. Radiat. Biol. Relat. Stud. Phys. Chem. Med. 49 (1986) 601–610.
[11] G.L. Griffiths, S.V. Govindan, G. Sgouros, G.L. Ong, D.M. Goldenberg, M.J. Mattes, Cytotoxicity with Auger electron-emitting radionuclides delivered by antibodies, Int. J. Cancer 81 (1999) 985–992.
[12] L. Yasui, A. Hughes, E. DeSombre, Relative biological effectiveness of accumulated ^{125}IdU- and ^{125}I-estrogen-decays in estrogen receptor-expressing MCF-7 human breast cancer cells, Radiat. Res. 155 (2001) 328–334.
[13] O.A. Sedelnikova, I.G. Panyutin, A.N. Luu, M.W. Reed, T. Licht, M.M. Gottesman, R.D. Neumann, Targeting the human mdr1 gene by ^{125}I-labeled triplex-forming oligonucleotides, Antisense Nucleic Acid Drug Dev. 10 (2000) 443–452.
[14] P.C. Chan, E. Lisco, H. Lisco, S.J. Adelstein, The radiotoxicity of iodine-125 in mammalian cells II. A comparative study on cell survival and cytogenetic responses to ^{125}IUdR, ^{131}TUdR, and ^{3}HTdR, Radiat. Res. 67 (1976) 332–343.
[15] R.E. Krisch, R.D. Ley, Induction of lethality and DNA breakage by the decay of iodine-1 in bacteriophage T4, Int. J. Radiat. Biol. Relat. Stud. Phys. Chem. Med. 25 (1974) 21–30.
[16] P.K. LeMotte, J.B. Little, DNA damage induced in human diploid cells by decay of incorporated radionuclides, Cancer Res. 44 (1984) 1337–1342.
[17] O.A. Sedelnikova, E.P. Rogakou, I.G. Panyutin, W.M. Bonner, Quantitative detection of (125) IdU-induced DNA double-strand breaks with gamma-H2AX antibody, Radiat. Res. 158 (2002) 486–492.
[18] L.S. Yasui, GammaH2AX foci induced by gamma rays and ^{125}IdU-decay, Int. J. Radiat. Biol. 80 (2004) 895–903.
[19] K. Datta, M. Dizdaroglu, P. Jaruga, R.D. Neumann, T.A. Winters, Enzymatic probing and structural mapping of a site-specific complex radiation-induced DNA double-strand break, I, J. Radiat. Oncol. Biol. Phys. 57 (2003), 1.
[20] K. Datta, R.D. Neumann, T.A. Winters, Characterization of a complex ^{125}I-induced DNA double-strand break: implications for repair, Int. J. Radiat. Biol. 81 (2005) 13–21.
[21] A.I. Kassis, Molecular and cellular radiobiological effects of Auger emitting radionuclides, Radiat. Prot. Dosim. 143 (2011) 241–247.
[22] S. Sundell-Bergman, R. Bergman, K.J. Johanson, Chromosome damage induced by decay of ^{3}H and ^{125}I incorporated into DNA of Chinese hamster cells, Mutat. Res. 149 (1985) 257–263.
[23] M. Hada, A.G. Georgakilas, Formation of clustered DNA damage after high-LET irradiation: a review, J. Radiat. Res. 49 (2008) 203–210.
[24] V. Dahmen, R. Kriehuber, Cytotoxic effects and specific gene expression alterations induced by I-125-labeled triplex-forming oligonucleotides, Int. J. Radiat. Biol. 88 (2012) 972–979.
[25] K.G. Hofer, N. van Loon, M.H. Schneiderman, D.E. Charlton, The paradoxical nature of DNA damage and cell death induced by 125I decay, Radiat. Res. 130 (1992) 121–124.
[26] S. Ritter, E. Nasonova, Y. Furusawa, K. Ando, Relationship between aberration yield and mitotic delay in human lymphocytes exposed to 200 MeV/u Fe-ions or X-rays, J. Radiat. Res. 43 (Suppl) (2002) S175–S179.
[27] R. Lee, E. Nasonova, S. Ritter, Chromosome aberration yields and apoptosis in human lymphocytes irradiated with Fe-ions of differing LET, Adv. Space Res. 35 (2005) 268–275.
[28] S. Ritter, M. Durante, Heavy-ion induced chromosomal aberrations: a review, Mutat. Res. 701 (2010) 38–46.
[29] J.P. Banath, S.H. Macphail, P.L. Olive, Radiation sensitivity, H2AX phosphorylation, and kinetics of repair of DNA strand breaks in irradiated cervical cancer cell lines, Cancer Res. 64 (2004) 7144–7149.
[30] S. Wada, T. Van Khoa, Y. Kobayashi, T. Funayama, K. Ogihara, S. Ueno, N. Ito, Prediction of cellular radiosensitivity from DNA damage induced by gamma-rays and carbon ion irradiation in canine tumor cells, J. Vet. Med. Sci. 67 (2005) 1089–1095.
[31] F. Tommasino, T. Friedrich, U. Scholz, G. Taucher-Scholz, M. Durante, M. Scholz, A DNA double-strand break kinetic rejoining model based on the local effect model, Radiat. Res. 180 (2013) 524–538.
[32] G.E. Pantelias, G.I. Terzoudi, Functional cell-cycle chromatin conformation changes in the presence of DNA damage result into chromatid breaks: a new insight in the formation of radiation-induced chromosomal aberrations based on the direct observation of interphase chromatin, Mutat. Res. 701 (2010) 27–37.
[33] G.I. Terzoudi, V.I. Hatzi, C. Donta-Bakoyianni, G.E. Pantelias, Chromatin dynamics during cell cycle mediate conversion of DNA damage into chromatid breaks and affect formation of chromosomal aberrations: biological and clinical significance, Mutat. Res. 711 (2011) 174–186.
[34] K. Elmroth, B. Stenerlow, Influence of chromatin structure on induction of double-strand breaks in mammalian cells irradiated with DNA-incorporated 125I, Radiat. Res. 168 (2007) 175–182.